Solid State Phenomena Vol. 160 (2010) pp 75-82
© (2010) Trans Tech Publications, Switzerland
doi:10.4028/www.scientific.net/SSP.160.75

Magnetic Quantitative Texture Analysis Using Isotropic Thermal Neutron Beams

D. Chateigner [a], B. Ouladdiaf [b] and F. Léon [a,b]

[a] CRISMAT-ENSICAEN, IUT-Caen, Université de Caen Basse-Normandie, Bd M. Juin, F-14050 Caen, France

[b] Institut Laue Langevin, Bd J. Horowitz, F-38042 Grenoble, France
daniel.chateigner@ensicaen.fr; ouladdiaf@ill.fr, francois.leon@ensicaen.fr

Keywords: Magnetic QTA, magnetic ODF

Abstract. We give the necessary formulas to extract pure magnetic diffraction signals from the difference spectra between two neutron texture measurements, one operated with a sample at zero-magnetic field, and the other under a magnetic field. This enables us to calculate the total-magnetic-scattering ODF, and the polarisation-magnetic-scattering ODF, of an iron sample. Using the developed approach it is shown that under some hypotheses one can describe the three dimensional orientation of the magnetic moments in the sample under a given magnetic field.

Introduction

Measuring magnetic pole figures using neutron diffraction is not new, but only few attempts of refining magnetic ODFs were carried out up to now. Among these the most successful work remains by Brisan *et al.* [1] using entropy maximisation to refine the ODF of a Fe(Si) compound, without consequent further development to our knowledge. However, the knowledge of the anisotropic distribution of magnetic moments in a sample has been proved to be of crucial importance to predict the macroscopic magnetic behaviour, for instance in ferromagnetic samples [2]. Anisotropic magnetic macroscopic behaviours are usually probed using magnetisation curves measured in two perpendicular macroscopic directions of the samples [3, 4]. However this kind of measurement is intrinsically subjected to strong biases if the sample magnetic moments distribution does not respect some symmetry, adapted to the magnetisation measurement. The magnetic moment distribution characterisation becomes then a prerequisite in order to check the validity of magnetisation measurements for a given sample-measurement configuration.

In this work we illustrate the capability of nonpolarised neutron beams in giving access to the spatial distribution of magnetic moments of a Fe sample subjected to a 0.3 T static magnetic field. The theoretical background of the methodology is described, and total-and polarisation magnetic-scattering ODFs refined to calculate the magnetic moment distribution.

Theoretical

Measured pole figures. For neutron diffraction, we observe pole figures, which are composed of a nuclear (n) and a magnetic (m) part, and in the pole figure space it writes, in zero-field or under application of an external magnetic field $\vec{B}$:

$$I_{\bar{h}}(\vec{y}) = I_{\bar{h}}^{n}(\vec{y}) + I_{\bar{h}}^{m}(\vec{y}) \qquad \text{and} \qquad I_{\bar{h}}(\vec{y},\vec{B}) = I_{\bar{h}}^{n}(\vec{y},\vec{B}) + I_{\bar{h}}^{m}(\vec{y},\vec{B}) \qquad (1)$$

If the crystallites are not free to rotate under the magnetic field, *e.g.* at solid state without phase transformation under field, we can assume:

$$I_{\bar{h}}^{n}(\vec{y},\vec{B}) = I_{\bar{h}}^{n}(\vec{y}), \qquad \text{hence,} \qquad I_{\bar{h}}(\vec{y},\vec{B}) = I_{\bar{h}}^{n}(\vec{y}) + I_{\bar{h}}^{m}(\vec{y},\vec{B})$$

This latter equation is of interest, because it can serve the determination of the magnetic part from an independent determination of the nuclear part, *e.g.* using x-ray diffraction.

Normalisation conditions of the pole figures. If complete pole figures are measured like with neutron experiments, the total intensity received on a given pole figure is:

$$\int_{\vec{y}} I_{\vec{h}}(\vec{y},\vec{B})dy \qquad \text{with } dy = \sin\vartheta_{\vec{y}}\, d\theta_{\vec{y}}\, d\varphi_{\vec{y}}$$

$$\int_{\vec{y}} I_{\vec{h}}(\vec{y},\vec{B})dy = \int_{\vec{y}} I^{n}_{\vec{h}}(\vec{y})dy + \int_{\vec{y}} I^{m}_{\vec{h}}(\vec{y},\vec{B})dy \qquad \text{for crystallites not free to rotate, or:}$$

$$\int_{\vec{y}} I_{\vec{h}}(\vec{y},\vec{B})dy = \int_{\vec{y}} I^{n}_{\vec{h}}(\vec{y},\vec{B})dy + \int_{\vec{y}} I^{m}_{\vec{h}}(\vec{y},\vec{B})dy \qquad \text{for free crystallites.} \qquad \textbf{(2)}$$

Since each contribution to $I_{\vec{h}}(\vec{y},\vec{B})$ has its own ODF, both $I^{n}_{\vec{h}}(\vec{y})$ (or $I^{n}_{\vec{h}}(\vec{y},\vec{B})$) and $I^{m}_{\vec{h}}(\vec{y},\vec{B})$ have to obey the normalisation condition:

$$\int_{\vec{y}} P^{n}_{\vec{h}}(\vec{y},\vec{B})dy = 2\pi \qquad \int_{\vec{y}} P^{m}_{\vec{h}}(\vec{y},\vec{B})dy = 2\pi$$

Hence the normalisation factors for the pole figures, or random intensities are:

$$I^{n,r}_{\vec{h}} = \frac{\int_{\vec{y}} I^{n}_{\vec{h}}(\vec{y},\vec{B})dy}{\int_{\vec{y}} dy}, \text{ and} \qquad I^{m,r}_{\vec{h}} = \frac{\int_{\vec{y}} I^{m}_{\vec{h}}(\vec{y},\vec{B})dy}{\int_{\vec{y}} dy} = I^{m,r}_{\vec{h}}(\vec{y},0) = I^{m,r}_{\vec{h}}(\vec{y},\vec{B}) \qquad \textbf{(3)}$$

Nuclear part determination. If one can find neutron peaks without magnetic contribution (only nuclear), several nuclear (crystallographic) characteristics can be determined:

- The full ODF of the nuclear part, or crystallographic texture (nODF = $f_n(g)$), can be determined, provided enough ODF space coverage is brought, by the only nuclear pole figures information. In this case, $f_n(g)$ can be used to recalculate all the $I^{n}_{\vec{h}}(\vec{y})$ contributions, and subtract them from $I_{\vec{h}}(\vec{y},\vec{B})$ to obtain the purely magnetic contributions. This implies the knowledge of the nuclear normalising factors of pole figures, $I^{n,r}_{\vec{h}}$. These latter can be obtained using:
  $I^{n,r}_{\vec{h}} = \dfrac{I^{n}_{\vec{h}}(\vec{y},\vec{B})}{P^{n}_{\vec{h}}(\vec{y},\vec{B})}$, $P^{n}_{\vec{h}}(\vec{y},\vec{B})$ being the recalculated normalised pole figures from $f_n(g)$.
- The following relation stands on each of these peaks:

  $$\int_{\vec{y}} I_{\vec{h}}(\vec{y},\vec{B})dy = \int_{\vec{y}} I^{n}_{\vec{h}}(\vec{y},\vec{B})dy$$

  which enables the calculation of $\int_{\vec{y}} I^{n}_{\vec{h}}(\vec{y},\vec{B})dy$ for any $\vec{h}$ pole figure, knowing the structure factors and experimental calibrations of the instrument (This is then in fact the ratio between the lines of a powder pattern).

The first approach works whatever the nuclear texture of the sample, and whatever the coverage of the pole figures (provided enough is provided to ensure the calculation of $f_n(g)$), while the second only works for a random crystallographic texture since the integral on $\vec{y}$ is constant only if all the poles have been measured, and in the case of complete pole figure measurements.

Normalisation conditions of the ODFs. We correlatively obtain the two ODFs, $f_n(g)$ and $f_m(g)$, that obey the normalisation conditions:

$$\int_g f_n(g)dg = 4\pi^2 \qquad \text{and} \qquad \int_g f_m(g)dg = 4\pi^2$$

Absence of external magnetic field. If B = 0, (1) and (2) become respectively:

$$I_{\bar{h}}(\vec{y},0) = I_{\bar{h}}^{n}(\vec{y},0) + I_{\bar{h}}^{m}(\vec{y},0) = I_{\bar{h}}^{n}(\vec{y}) + I_{\bar{h}}^{m}(\vec{y},0) \quad (4)$$

$$\int_{\bar{y}} I_{\bar{h}}(\vec{y},0)dy = I_{\bar{h}}^{n,r} + I_{\bar{h}}^{m,r} \quad (5)$$

In (5), the ratio between $I_{\bar{h}}^{n,r}$ and $I_{\bar{h}}^{m,r}$ is given by any program able to calculate magnetic and nuclear powder patterns (Fullprof, Jana, GSAS …).

Whether $I_{\bar{h}}^{m}(\vec{y},0)$ is anisotropic or not depends on many factors, on the magnetic moments configuration in the unit cell, on the crystallographic texture, on the magnetic behaviour (spontaneous magnetic polarisation), on the sample history … For now we can dissociate four different initial sample configurations in zero external field (Table 1).

Initial Sample	Random texture	Textured
Magnetic Isotropy	Isotropic	Textured isotropic
Magnetic Anisotropy	Isotropised	Anisotropic

Table 1: Definitions of sample configurations in absence of applied magnetic field

Application of an external magnetic field. The application of a field $\vec{B}$ induces eventually a reorientation of magnetic moments in the sample, or magnetic polarisation, which is seen using neutron diffraction as variations of intensities, $\Delta I_{\bar{h}}^{m}(\vec{y},\vec{B})$, in the pole figures, and (1) becomes:

$$I_{\bar{h}}(\vec{y},\vec{B}) = I_{\bar{h}}^{n}(\vec{y},\vec{B}) + I_{\bar{h}}^{m}(\vec{y},0) + \Delta I_{\bar{h}}^{m}(\vec{y},\vec{B}) \quad (6)$$

We will call these variations in intensities of the pole figures under magnetic field, magnetic-scattering polarisation pole figures. These variations are positive or negative. Then, compared to (1), the measured pole figure will exhibit y-ranges where intensities will appear reinforced, and some other y-ranges for which the intensities will be lowered.

Since the applied field can reorient the magnetic moments or destroy their initial orientations, and depending on the magnitude of the applied field, each initial state of Table 1 splits into 2 possible configurations (isotropic or not) after the field is applied. For instance, an initially ferromagnetic isotropic sample will remain isotropic after magnetic field application if this field is smaller than the coercive field, while will become magnetically anisotropic if $B > B_c$ (Table 2), resulting in eight possible sample histories, but only four sample final states after field application.

Initial Sample	Random texture	Textured
Magnetic Isotropy	Isotropic Magnetically anisotropic	Textured isotropic Anisotropic
Magnetic Anisotropy	Isotropic Magnetically anisotropic	Anisotropic Textured isotropic

Table 2: Resulting possible sample states after application of a magnetic field

Magnetic part determination. There are two different magnetic pole figures one can obtain: the magnetic-scattering polarisation pole figures, $\Delta I_{\bar{h}}^{m}(\vec{y},\vec{B})$, and the total magnetic-scattering pole figures, $I_{\bar{h}}^{m}(\vec{y},\vec{B})$, with:

$$I_{\bar{h}}^{m}(\vec{y},\vec{B}) = I_{\bar{h}}^{m}(\vec{y},0) + \Delta I_{\bar{h}}^{m}(\vec{y},\vec{B}) \qquad (7)$$

Magnetic polarisation pole figures. Under magnetic field, the magnetic-scattering polarisation pole figures can be obtained straightforwardly by taking the difference between (6) and (4):

$$\Delta I_{\bar{h}}^{m}(\vec{y},\vec{B}) = I_{\bar{h}}(\vec{y},\vec{B}) - I_{\bar{h}}(\vec{y},0) \qquad (8)$$

whatever the crystallographic texture $I_{\bar{h}}^{n}(\vec{y})$ and the initial magnetic state $I_{\bar{h}}^{m}(\vec{y},0)$.

One can see straightforwardly, that if the magnetic field imposes crystallite reorientations, then:

$$I_{\bar{h}}(\vec{y},\vec{B}) - I_{\bar{h}}(\vec{y},0) = I_{\bar{h}}^{n}(\vec{y},\vec{B}) + I_{\bar{h}}^{m}(\vec{y},0) + \Delta I_{\bar{h}}^{m}(\vec{y},\vec{B}) - I_{\bar{h}}^{n}(\vec{y},0) - I_{\bar{h}}^{m}(\vec{y},0)$$
$$= I_{\bar{h}}^{n}(\vec{y},\vec{B}) + \Delta I_{\bar{h}}^{m}(\vec{y},\vec{B}) - I_{\bar{h}}^{n}(\vec{y},0)$$

and (8) becomes:

$$\Delta I_{\bar{h}}^{m}(\vec{y},\vec{B}) = I_{\bar{h}}(\vec{y},\vec{B}) - I_{\bar{h}}(\vec{y},0) + I_{\bar{h}}^{n}(\vec{y},0) - I_{\bar{h}}^{n}(\vec{y},\vec{B})$$

so that we need to know how the crystals reorient under a magnetic field. This is hopefully often negligible. If not, this is another matter not dealt here.

Total magnetic-scattering pole figures. The total magnetic-scattering contribution to a given pole figure (7) requires the determination of $I_{\bar{h}}^{m}(\vec{y},0)$ and $\Delta I_{\bar{h}}^{m}(\vec{y},\vec{B})$. The latter term is obtained using (8). But the former term determination needs to distinguish between two possible initial magnetic states:

Initially magnetically isotropic sample

In this case we get $I_{\bar{h}}^{n}(\vec{y},0)/I_{\bar{h}}^{m}(\vec{y},0) = \text{constant} = A, \forall\, \vec{y}$. The constant A can be calculated from a powder pattern measured in the same conditions as the pole figures (or refined in a Rietveld approach if a software is available to treat both magnetic and nuclear patterns and ODFs), for instance using Fullprof. Then, dividing (1) by $I_{\bar{h}}^{m}(\vec{y},0)$, one gets $I_{\bar{h}}(\vec{y},0)/I_{\bar{h}}^{m}(\vec{y},0) = I_{\bar{h}}^{n}(\vec{y},0)/I_{\bar{h}}^{m}(\vec{y},0) + 1 = 1 + A$, which allows the calculation of the total magnetic-scattering contribution from the measured pole figures and A.

Initially magnetically anisotropic sample

In this case $I_{\vec{h}}^{m}(\vec{y},0) \neq I_{\vec{h}}^{m,r}$, and we then need to determine it from (4):

$$I_{\vec{h}}^{m}(\vec{y},0) = I_{\vec{h}}(\vec{y},0) - I_{\vec{h}}^{n}(\vec{y},0)$$

$I_{\vec{h}}^{n}(\vec{y},0)$ has then to be determined using non-magnetic peaks.

Furthermore, if one uses the fact that:

$$I_{\vec{h}}(\vec{y},\vec{B}) - I_{\vec{h}}^{n}(\vec{y},0) = I_{\vec{h}}^{n}(\vec{y},\vec{B}) + I_{\vec{h}}^{m}(\vec{y},\vec{B}) - I_{\vec{h}}^{n}(\vec{y},0),$$

without solid state crystal reorientation, $I_{\vec{h}}^{n}(\vec{y},0) = I_{\vec{h}}^{n}(\vec{y},\vec{B})$, and the full magnetic contribution is:

$$I_{\vec{h}}^{m}(\vec{y},\vec{B}) = I_{\vec{h}}(\vec{y},\vec{B}) - I_{\vec{h}}^{n}(\vec{y},0)$$

From magnetic-scattering to the MODF and magnetic moment distributions.

The magnetic-scattering pole figures (polarisation and total) are a direct consequence of the interaction of neutrons with magnetic moments (in their reoriented or initial states respectively). However, the magnetic moment distribution is not directly given by the magnetic-scattering pole figures. One needs to take into account how the magnetic moment scatter neutrons. The neutron-magnetic moment interaction involves a vector product, meaning that for an intensity detected at g, the real magnetic moment orientation is at 90° from g, taking into account time reversal symmetry relationships. In the case of magnetic moments linked to crystallographic directions, this is quite straightforward [2], but this is not unfortunately always the case, as for a soft magnetic material. However, magnetic unit-cell parameters are usually linked to the unit-cell of the nuclear part of the sample, and once enough magnetic pole figures $I_{\vec{h}}^{m}(\vec{y},\vec{B})$ have been extracted, $f_m(g)$ can be refined using the rotation part of the magnetic space group, as for a classical crystallographic f(g), in any QTA software. We used here the tetragonal magnetic representation in order to account for the dissociation of [100] and [001] directions, to which the magnetic moments can be aligned.

Experimental

We used the newly developed curved area position sensitive detector of the D19 beamline for our measurements [5]. This detector has the peculiarity of a χ-equivalent opening angle of 30° on 120° in 2θ, which strongly economises measuring time (only 288 sample orientations are necessary to cover all complete pole figures). Furthermore the D19 beamline is located close to the ILL reactor, with a large incident flux on the sample. Taking these technical advantages into account, it becomes feasible to operate two successive QTA measurements, one without applied magnetic field on the sample, and the other with a field of 0.3 T. We developed a sample holder, which enables to apply the magnetic field without dismounting the sample, and which is fixed in the sample reference frame when this latter rotates in the Eulerian cradle. The moderate applied field magnitudes (provided by the insertion of a Nd-Fe-B permanent magnet) however allow at the present time to characterise only samples under low fields, and this is the reason why we measured an iron cylinder.

Results and discussion

From the two measurement sets (without and with applied field, Figure 1), we applied the previously described procedure to carry out total and polarisation magnetic-scattering complete {110} pole figures. The magnetic form factors are such that only the {110} line exhibits enough magnetic information in our conditions. At zero field (Figure 2a) the sample exhibits a strong signal with a moderate <110> crystallographic texture. When a field of 0.3 T is applied (Figure 2b), the maximum of the {110} experimental pole figure decreases significantly at the benefit of the pole figure equator. This is coherent with a magnetic field applied along the sample cylinder axis (Z_S, centre of the pole figures), to which magnetic moments tend to align, giving rise to more magnetic diffraction signal at 90° from it. The difference {110} pole figure illustrates this more explicitly (Figure 2c), with negative differences on its centre and positive values on its equator.

We then calculated the random magnetic contribution (A) of the isotropic magnetic sample using Fullprof (Figure 2d), using the sum of all diagrams measured at all the sample orientations, taking into account the D19 instrument resolution characteristics. This random magnetic contribution provides the possibility to dissociate nuclear and magnetic contributions at zero field, $I_{\vec{h}}^{n}(\vec{y},0)$ and $I_{\vec{h}}^{m}(\vec{y},0)$ respectively.

These latter pole figures were used to refine the corresponding ODFs, $f_n(g)$ and $f_m(g)$, using the bcc crystal symmetry and the orthorhombic magnetic symmetries respectively, and the WIMV algorithm of Beartex [6]. In order to refine $f_m(g)$, we declared the overlaps refined by Fullprof to take account of the multiplicity of the {110} magnetic pole figure. The nuclear <110> fibre texture (Figure 2e) culminates at 1.32 mrd ($f_n^{max}(g)$=1.8mrd, $f_n^{min}(g)$=0.61mrd, F^2=1.03mrd^2, RP0=1.42%), and the fibre axis is aligned with Z_S, as the sole textured component (Figure 2f). Since in iron the easy axis direction for magnetisation is <100>, the actual <110> fibre does not correspond to an easy magnetisation configuration. Consequently, the total normalised magnetic-scattering pole figures of the main magnetic unit-cell axes (Figure 2g) do not show a strong reorientation of densities, and exhibit a maximum of 1.32 mrd only on the pole figures, but a larger ODF maximum value ($f_n^{max}(g)$ = 2.3mrd, $f_n^{min}(g)$ = 0.64mrd, F^2 = 1.03mrd^2, RP0 = 0.24%).

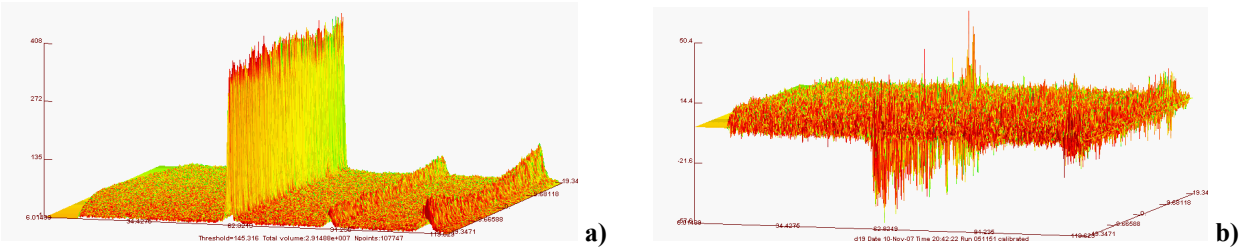

Figure 1: One 2D Debye-Scherrer pattern for one sample orientation without field (left) and difference pattern for the corresponding sample orientation (right).

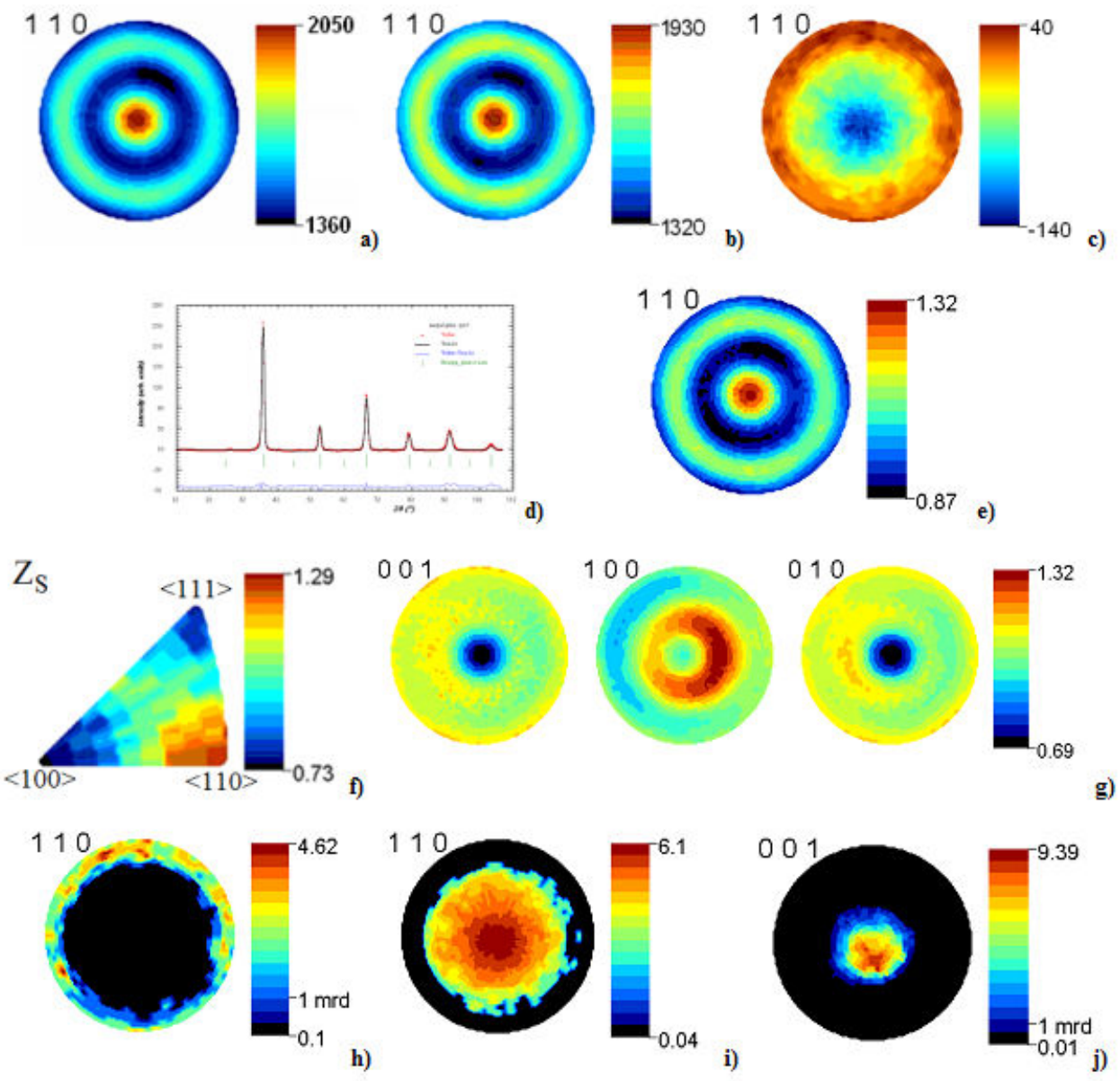

Figure 2: {110} pole figures at zero field (**a**), under 0.3 T (**b**) and difference (**c**). Fit of the sum of all diagrams at zero field using the orthorhombic magnetic sub-group in Fullprof (**d**), and WIMV recalculated-normalised nuclear {110} pole figure (**e**). Inverse nuclear pole figure for the cylinder sample axis direction (**f**) and WIMV recalculated-normalised magnetic-scattering contribution for the main orthorhombic axes (**g**). Recalculated-normalised magnetic-scattering polarisation pole figures for the positive (**h**) and negative (**i**) parts of the difference pole figures, and corresponding positive {001} magnetic-scattering pole figure illustrating the magnetic moment reorientation (**j**).

From the magnetic-scattering polarisation pole figures we refined the magnetic polarisation ODF, $\Delta f_m(g)$. Since the magnetic-scattering difference pole figures are showing positive and negative values, we divided them into their positive and negative zones, $\Delta I_{\vec{h}}^{+m}(\vec{y},\vec{B})$ and $\Delta I_{\vec{h}}^{-m}(\vec{y},\vec{B})$ respectively, assigning zeros to the negative cells of $\Delta I_{\vec{h}}^{+m}(\vec{y},\vec{B})$ and vice-versa. From $\Delta I_{\vec{h}}^{+m}(\vec{y},\vec{B})$ and $\left|\Delta I_{\vec{h}}^{-m}(\vec{y},\vec{B})\right|$ we refined the magnetic-scattering polarisation ODFs, $\Delta f_{+m}(g)$ ($f_n^{max}(g)$ = 93mrd, $f_n^{min}(g)$ = 0mrd, F^2 = 12.4mrd^2, RP0 = 6.83%) and $\Delta f_{-m}(g)$ ($f_n^{max}(g)$ = 6.1mrd, $f_n^{min}(g)$ = 0.04mrd, F^2=2.70mrd^2, RP0 = 0.00%) in Beartex, which gave back the normalised $\Delta P_{110}^{+m}(\vec{y},\vec{B})$ and $\left|\Delta P_{110}^{-m}(\vec{y},\vec{B})\right|$ pole figures (Figure 2h and i resp.). These latter clearly show the reoriented part of the

magnetic signal with a large density created in the centre of $\left|\Delta P_{110}^{-m}(\vec{y},\vec{B})\right|$ indicating departure of intensities in this area to reach the periphery of $\Delta P_{110}^{+m}(\vec{y},\vec{B})$, both pointing toward magnetic moment alignment with Z_S. The maximum densities observed on these latter pole figures somehow measure the strength of the intensity reorientations, as also seen from texture indexes and ODF maxima. Most importantly, since the diffracted signal reveals magnetic moments located at 90° from it, one can search in this case a reflection at this angle from 110, which is for instance 001 in this space group. The $\Delta P_{001}^{+m}(\vec{y},\vec{B})$ (Figure 2j) then reveals directly the reoriented magnetic moments distribution, which in this case points a 9.4 mrd density of the reorientation. Interestingly in this case one can see a slight but significant deviation of these magnetic moments with respect with Z_S (<110> crystallographic fibre axis), probably due to the difficulty to control our magnetic field application.

Conclusions

We have shown the possibility of working out directly, using difference pole figures, the visualisation of magnetic moment reorientation, using classical ODF refinement methods. The measurements need optimised neutron beams and detecting tools in order to work out two texture measurement sets in reasonable times, for revealing the magnetic signals accurately using nonpolarised neutrons. Using this approach, the total magnetic-scattering ODF can be accessed, but also the magnetic-scattering polarisation ODF. Magnetic moments distribution and reorientation can be detailed quantitatively in three dimensions.

References

[1] M. Birsan, J.A. Szpunar, Z. Tun and J.H. Root: Magnetic texture determination using nonpolarized neutron diffraction. Physical Review B Vol. **53(10)** (1996), p. 6412-6417

[2] M. Morales, D. Chateigner and D. Fruchart: Texture and magneto-crystalline anisotropy analysis of an oriented $ErMn_4Fe_8C$ powder sample. Journal of Magnetism and Magnetic Materials Vol. **257(2)** (2003), p. 258-269

[3] J.-G. Noudem, J. Beille, D. Bourgault, D. Chateigner and R. Tournier: Bulk textured Bi-Pb-Sr-Ca-Cu-O (2223) ceramics by solidification in a magnetic field. Physica C Vol. **264** (1996), p. 325-330

[4] B. Legrand, D. Chateigner, R. Perrier de la Bathie and R. Tournier: Orientation by solidification in a magnetic field: a new process to texture SmCo compounds used as permanent magnets. J. Magnetism and Magnetic Materials Vol. **173** (1997), p. 20-28

[5] F. Léon, D. Chateigner, B. Ouladdiaf, L. Lutterotti, M. Zucali and D. Richard: Neutron Quantitative texture analysis using 120° curved area PSD at D19-ILL. *Submitted to* Journal of Applied Crystallography. (2009).

[6] H.-R. Wenk, S. Matthies, J. Donovan and D. Chateigner: BEARTEX: A Windows based program for quantitative texture analysis. Journal of Applied Crystallography Vol. **31** (1998), p. 262-269